

## Supplementary Information

### Core-shell metal-organic frameworks and hierarchical host-guest structures toward water-stable luminescence of lanthanide complexes in encoding beads

Dong Mo, Zhengqiang Wang, Kaiyao Sun, Xiyue Xie, Jixi Zhang\*, Kaiyong Cai\*

Key Laboratory of Biorheological Science and Technology, Ministry of Education, College of Bioengineering, Chongqing University, No. 174 Shazheng Road, Chongqing 400044, China  
E-mail: jixizhang@cqu.edu.cn, kaiyong\_cai@cqu.edu.cn.

#### 1. Characterization

Transmission electron microscopy (TEM) images were performed on a JEM 2010 (JEOL, Japan) instrument with 200 kV acceleration voltages in order to investigate the size, morphology and integrity of nanoparticles. Samples were dried on holey carbon-coated Cu grids before characterization. The bulk and surface chemical compositions of samples were analyzed with HAADF-STEM (high-angle annular dark-field imaging, scanning transmission electron microscope) and elemental mapping images via a JEM-6700F instrument (JEOL, Japan).

Powder X-ray diffraction (XRD) measurements were obtained using Bruker D8 (Germany) Advance X-Ray powder diffractometer (40 kV, 40 mA, CuK $\alpha$ 1 radiation of  $\lambda = 1.54059 \text{ \AA}$ ) with a scan speed of  $2^\circ/\text{min}$  and a step size of  $0.02^\circ$ .

Nitrogen sorption isotherms were measured through an ASAP 2010 analyzer (Micromeritics, USA).

XPS analysis was determined by an Axis Ultra spectrometer (Kratos, UK) with Al K $\alpha$  excitation radiation at ca.  $5 \times 10^{-9} \text{ Pa}$ .

Fourier transform infrared (FTIR) spectra were recorded on a Spectrum 100 infrared spectrophotometer (PerkinElmer, USA) at a test range of  $400\text{-}4000 \text{ cm}^{-1}$  using the KBr pellet

technique.

The contact angles for water on the surfaces of the as-obtained particles films were carried out using a JY-PHa optical contact angle meter (JY-PHa, JinHe Machine, China) at room temperature. The values of contact angles were obtained within 20 s after depositing and drying 1 mL of particle suspension ( $15 \text{ mg mL}^{-1}$ ) on a titanium sheet.

Thermogravimetric analysis (TGA) was performed with a Q500 instrument (TA Instruments, USA). The samples were tested under an air atmosphere from  $25^\circ\text{C}$  to  $900^\circ\text{C}$  at a heating rate of  $10^\circ\text{C}/\text{min}$ .

The UV-vis absorption was recorded on a UV-Vis spectrofluorometer (NanoDrop One, Thermo). Fluorescence spectra was recorded on a fluorescence spectrophotometer (RF-6000, Shimadzu, Japan) using a xenon lamp as excitation source.

Fluorescence quantum yield (QY) was collected using an integrating sphere (FS5, Edinburgh Instruments), and the luminescence lifetime data were determined independently using a fluorescence spectrophotometer (FLS920, Edinburgh Instruments). The employed excitation wavelength was 304 nm and emission wavelength was 543 nm.

## 2. Supporting Figures

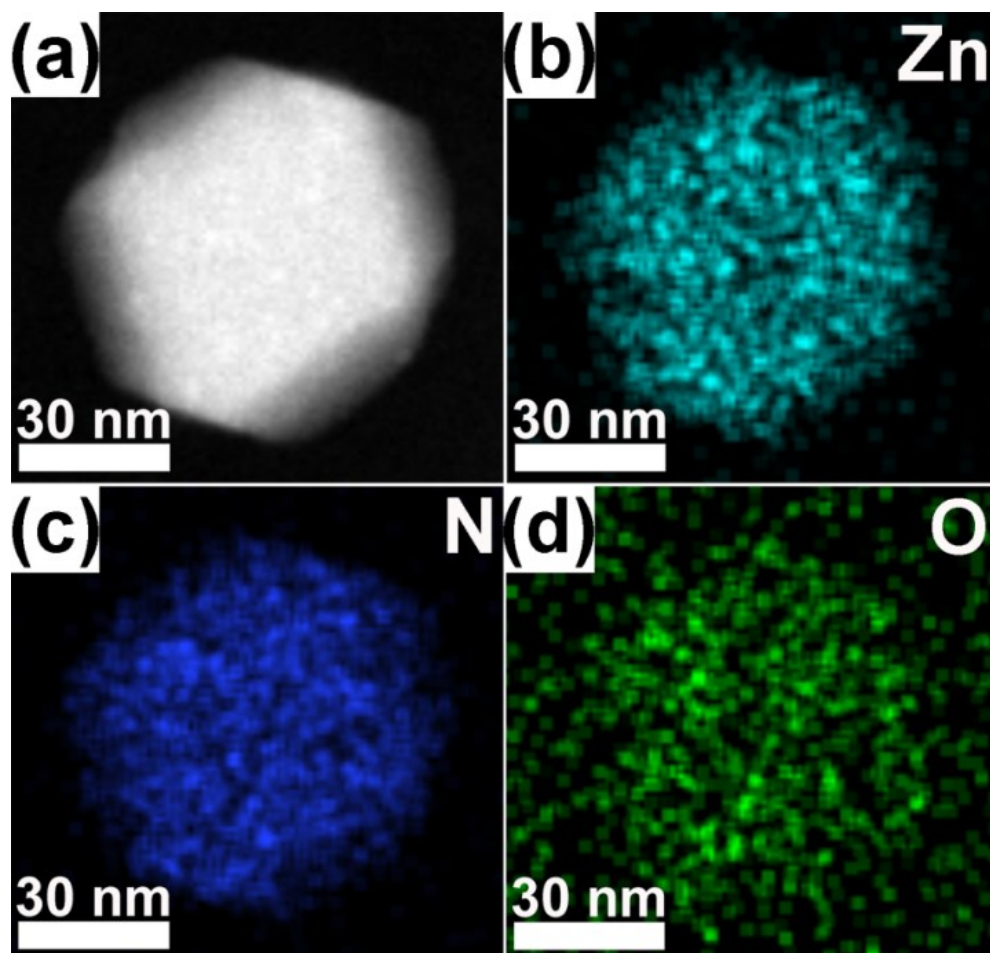


**Fig. S1** HAADF-STEM (a) and EDS mapping images (b, c, d) showing distributions of Tbx@ZIF-8@ZIF-90 NPs.

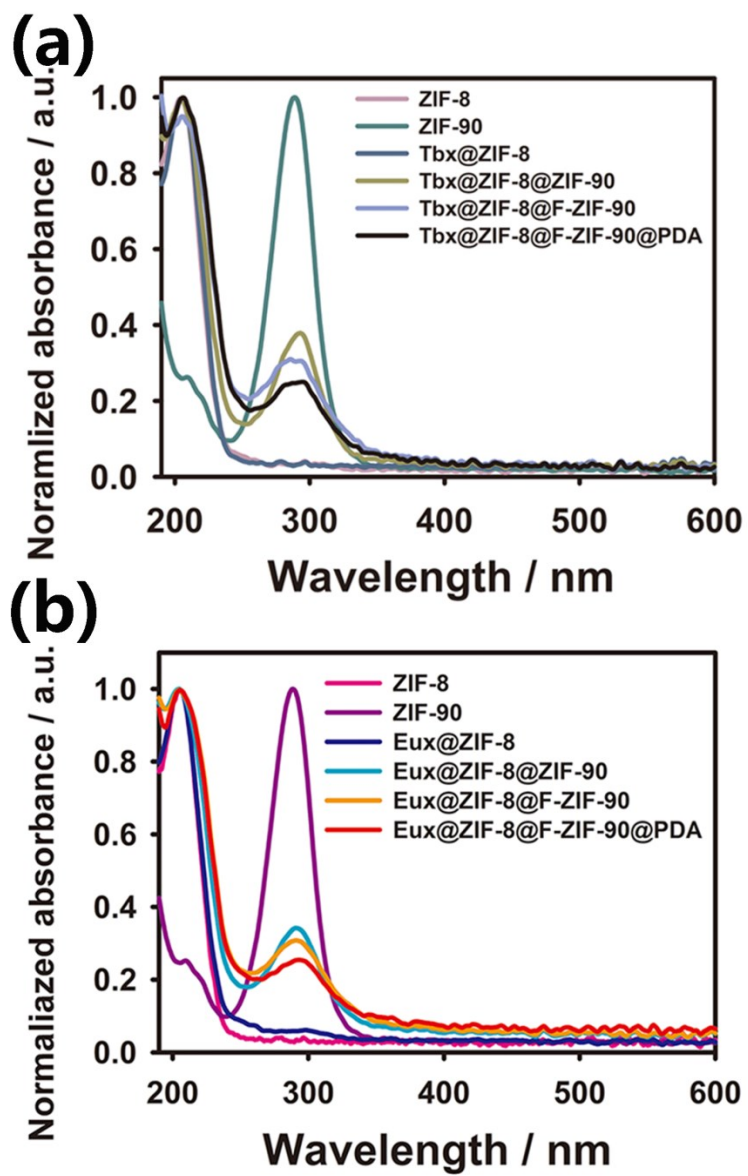
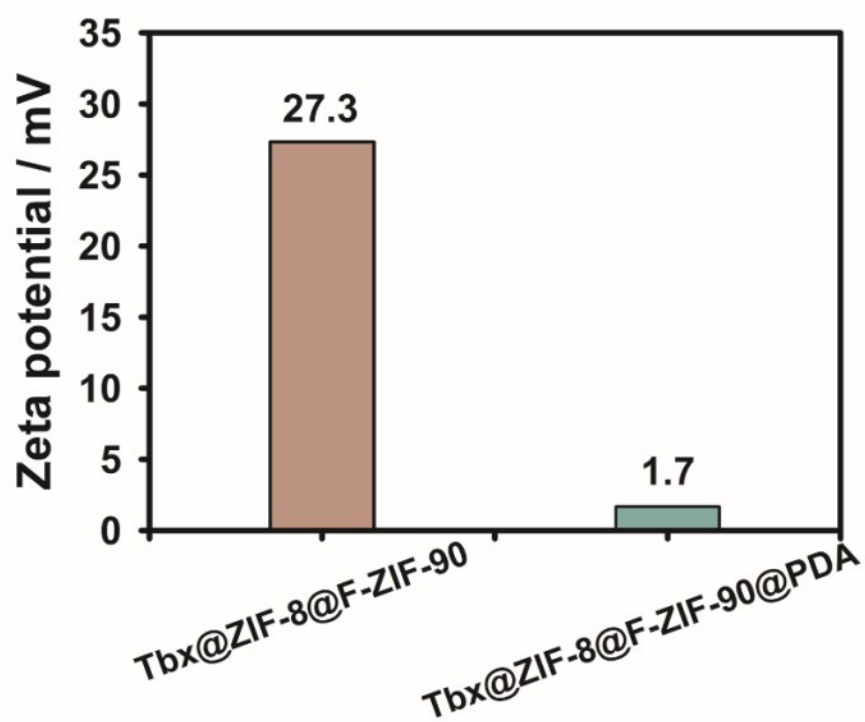
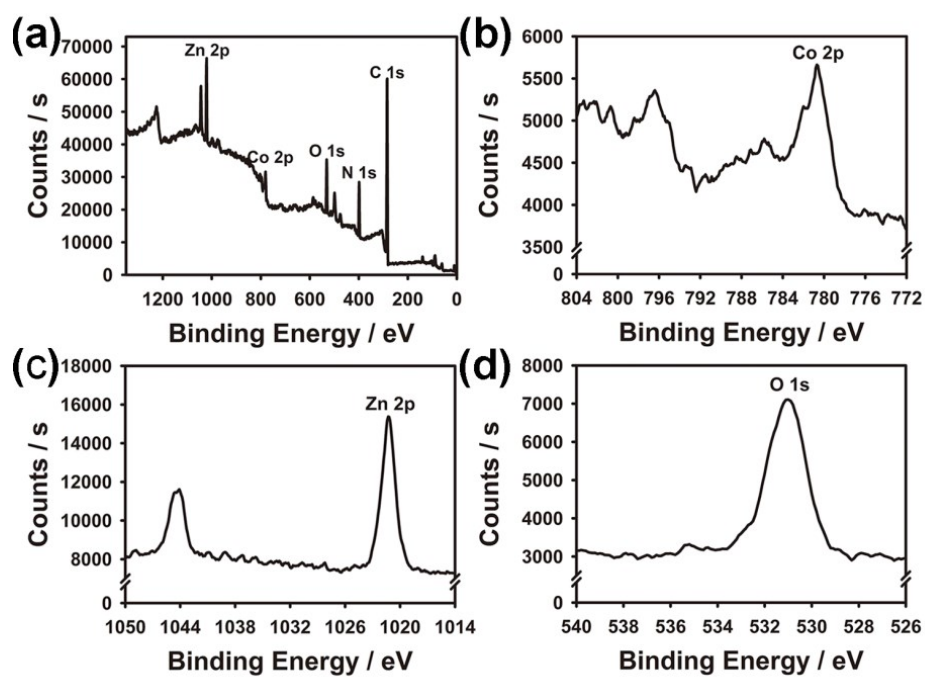


Fig. S2 Normalized UV-Vis absorption spectra of all optical particles coated Tb (a) or Eux (b), ZIF-90 NPs, and ZIF-8 NPs.



**Fig. S3** Zeta potential changes of Tbx@ZIF-8@ZIF-90 NPs and Tbx@ZIF-8@F-ZIF-90@PDA NPs.



**Fig. S4** XPS survey of ZIF-67@ZIF-90 NPs (a), and corresponding high-resolution scans of the Co 2p (b), Zn 2p (c), and O 1s (d) peak from the XPS spectra of nanoparticles.

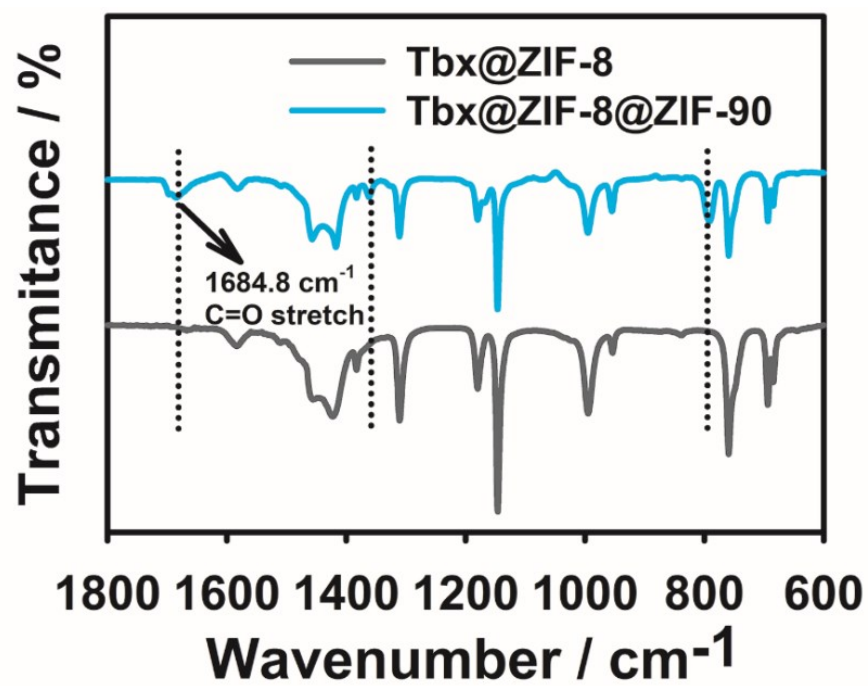
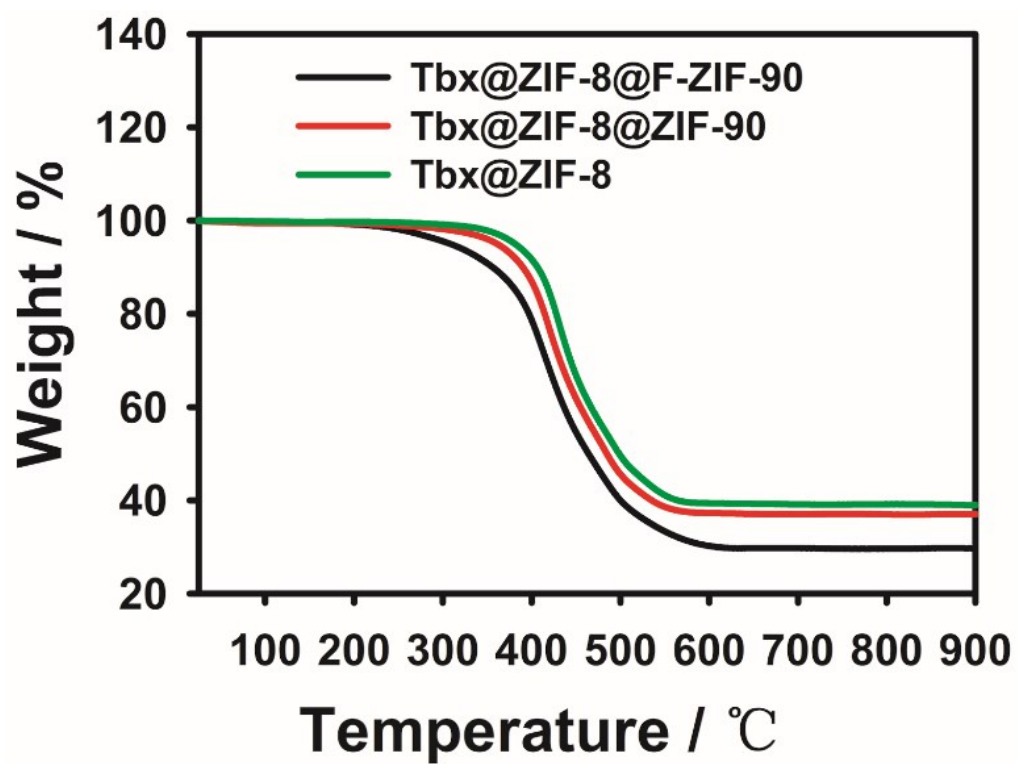
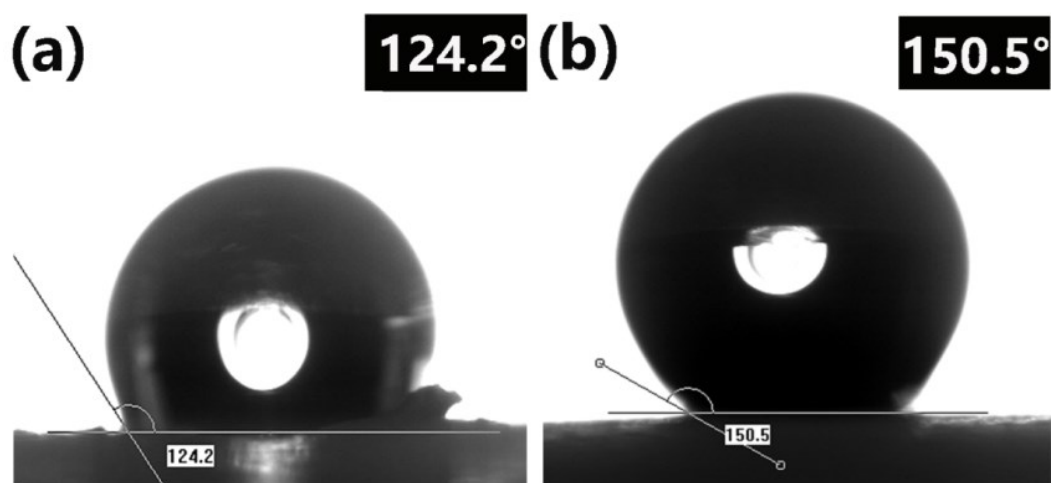


Fig. S5 FT-IR spectra of Tbx@ZIF-8 NPs and Tbx@ZIF-8@ZIF-90 NPs.



**Fig. S6** TGA curves of Tbx@ZIF-8 NPs (green line), Tbx@ZIF-8@ZIF-90 NPs (red line) and Tbx@ZIF-8@F-ZIF-90 NPs (black line).





**Fig. S7** Measurement of the contact angle with the water for Tbx@ZIF-8@F-ZIF-90 NPs: ZIF-90 shell by one-step synthesis (a) and F-ZIF-90 NPs (b); 2, 4, 6-trifluorobenzyl amine as fluorinating agent.

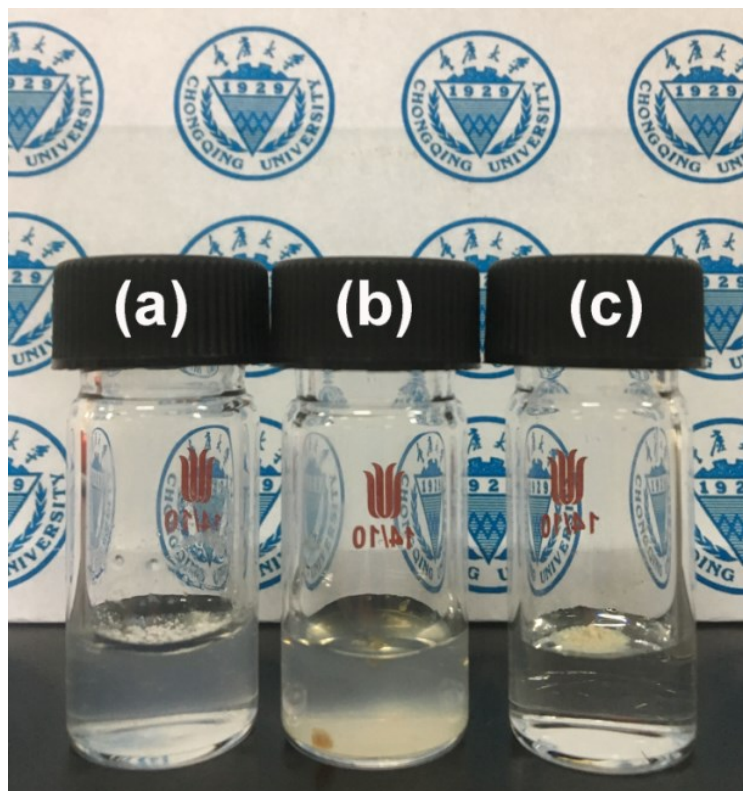


**Fig. S8** Digital photographs of Tbx@ZIF-8 (a), Tbx@ZIF-8@ZIF-90 (b), and Tbx@ZIF-8@F-ZIF-90 (c) samples dispersed in water solution.



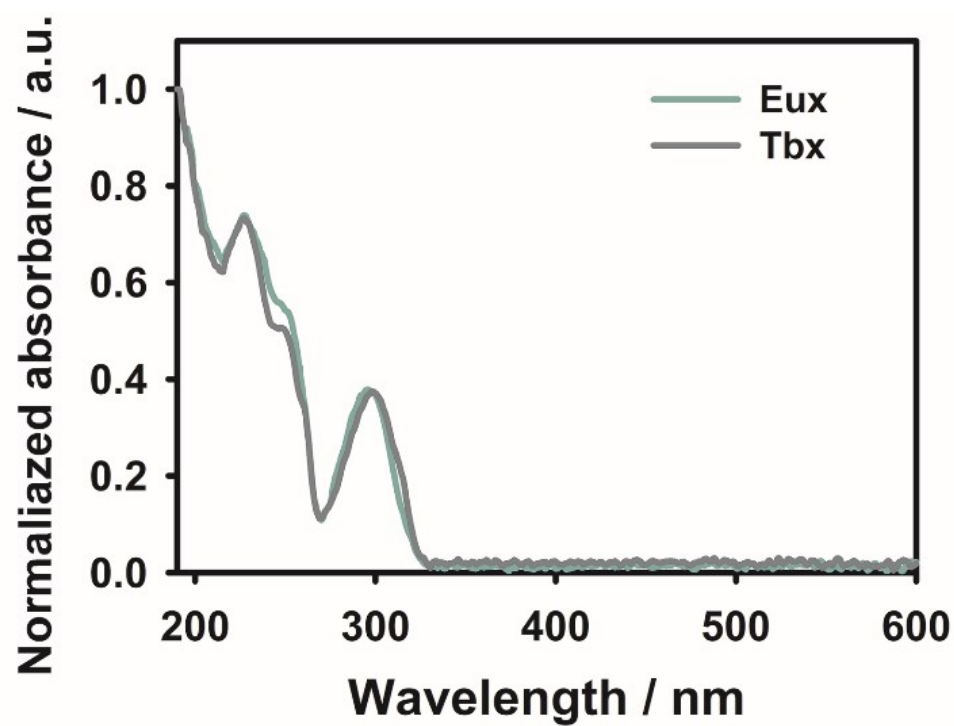
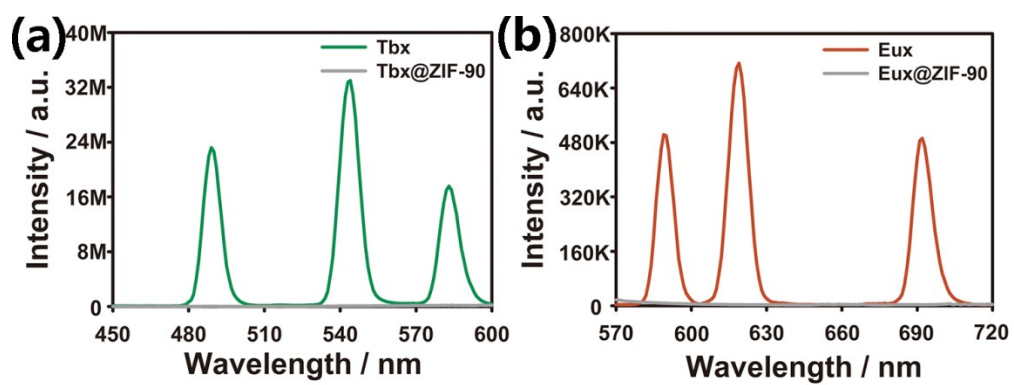


Fig. S10 Normalized UV-Vis absorption spectra of Eux and Tbx.



**Fig. S11** Photoluminescence spectra of Tb<sup>3+</sup> and Tb<sup>3+</sup>@ZIF-90 NPs (a); Eu<sup>3+</sup> and Eu<sup>3+</sup>@ZIF-90 NPs

(b).

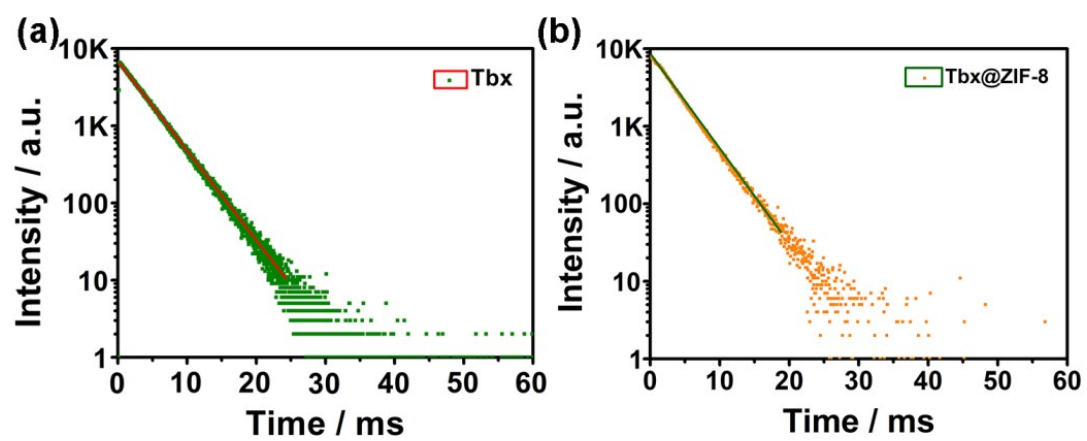
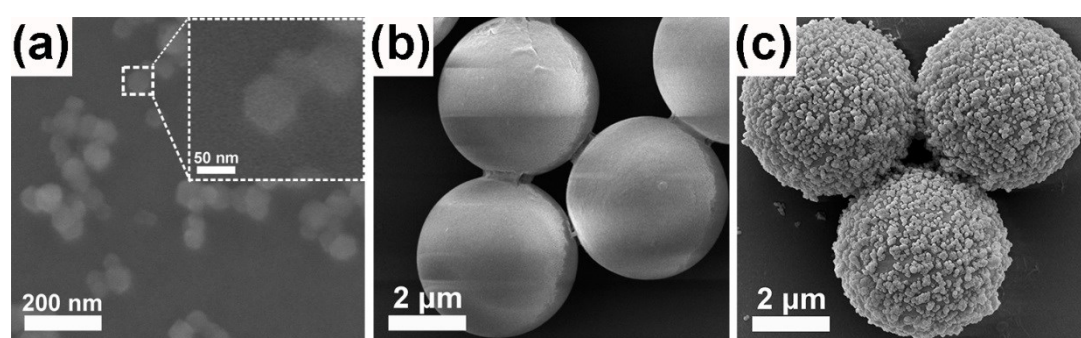
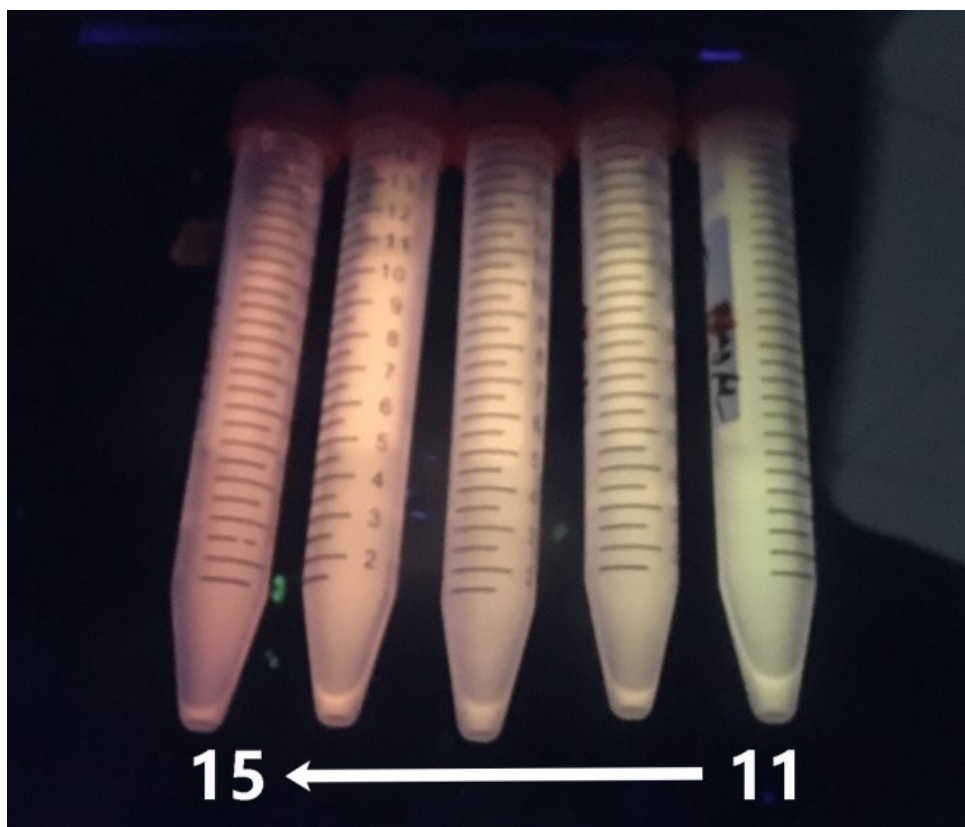


Fig. S12 Time-resolved luminescence decay curves of Tbx (a) and Tbx@ZIF-8 NPs (b).



**Fig. S13** SEM images of the non-fluorescent ZIF-8@F-ZIF-90@PDA NPs (a), NH<sub>2</sub>-PS (b) and fluorescent encoding beads (c) at medium magnification.



**Fig. S14** Digital photographs of DEBs dispersed in aqueous solution.



**Table S1** Summarized photophysical properties of the suspensions of Tbx, Tbx@ZIF-8 NPs and Tbx@ZIF-8@F-ZIF-90 NPs. Particles were suspended in PBS buffer (pH 7.4) at a fixed concentration of 0.1 mg mL<sup>-1</sup>.

Sample name	$\Phi^a_{\text{PBS}}/\%$	$\tau^b_{\text{PBS}}/\text{ms}$
Tbx	-	2.2
Tbx@ZIF-8	13.4	2.0
Tbx@ZIF-8@F-ZIF-90@PDA	19.1	1.8

**a:** Absolute luminescence QYs of particles suspended in PBS buffer (pH 7.4).

**b:** Lifetime  $\tau$  of particles suspended in PBS buffer (pH 7.4). The samples were freshly prepared in PBS and immediately utilized for QY and lifetime measurements.

**Table S2** Single-color encoding formula and the resulting fluorescence properties of EBs base on Tbx NPs and NF NPs.

SEBs	Tbx NPs %	NF NPs %	Fluorescence intensity (a.u.) 543 nm
1	100	0	3898
2	85	15	2921
3	70	30	1702
4	55	45	1143
5	40	60	760

**Table S3** Single-color encoding formula and the resulting fluorescence properties of EBs base on Eux NPs and NF NPs.

SEBs	Eux NPs %	NF NPs %	Fluorescence intensity (a.u.) 617 nm
6	100	0	3971
7	90	10	2706
8	80	20	1946
9	70	30	1526
10	60	40	997

**Table S4** Double-color encoding formula and the resulting fluorescence properties of EBs base on Tbx NPs, Eux NPs and NF NPs.

DEBs	Tbx NPs %	NF NPs %	Eux NPs %	Fluorescence intensity (a.u.)	
				543 nm	617 nm
11	22	48	30	3152	1056
12	19	36	45	2721	1470
13	16	24	60	2231	1894
14	13	12	75	1161	2463
15	10	0	90	1308	2804